International Journal of Scientific Research in Science and Technology
Print ISSN: 2395-6011 | Online ISSN: 2395-602X (www.ijsrst.com)
doi : https://doi.org/10.32628/IJSRST52310386

Automated Slice Thickness Measurement on the Nessoft CT QA Phantom

Rini Marini[1], Choirul Anam[1], Eko Hidayanto[1], Ariij Naufal[1], Geoff Dougherty[2]

[1]Departement of Physics, Faculty of Sciences and Mathematics, Diponegoro University, Jl. Prof. Soedarto SH, Tembalang, Semarang 50275, Central Java, Indonesia

[2]Department of Applied Physics and Medical Imaging, California State University Channel Islands, Camarillo, CA 93012, USA

ARTICLEINFO

Article History:

Accepted: 05 May 2023
Published: 29 May 2023

Publication Issue
Volume 10, Issue 3
May-June-2023

Page Number
472-484

ABSTRACT

Purpose: This study proposes a method for automatically measuring slice thickness on image of the Neusoft CT quality assurance (QA) phantom.

Method: The Neusoft CT QA phantom was scanned by a Neuviz 16-slice Neusoft CT Scanner. Automated measurement was implemented using IndoQCT software, while manual measurement was conducted using MicroDicom viewer as comparison. The system was evaluated on images with variations of slice thickness (i.e 1.25, 2.5, 3, 5, and 10 mm), tube voltage (i.e. 80,100,120, and 140 kV), and tube current (i.e. 77, 154, 231, and 233 mA).

Results: The results of automated slice thickness method for slice thicknesses of 1.25, 2.5, 3, 5, and 10 mm were 1.47 + 0.17, 2.67 + 0.08, 3.21 + 0.17, 5.21 + 0.13, and 10.95 + 0.28 mm, respectively. By comparison, the results of manual slice thickness method were 2.91 + 0.17, 3.28 + 0.29, 3.56 + 0.29, 4.72 + 0.27, and 11.35 + 2.03, respectively (p-value 0.009, 0.002, 0.047, 0.008, and 0.714). The results of automated method for tube voltages of 80,100,120, and 140 kV were 5.61 + 0.34, 5.12 + 0.23, 5.08 + 0.23, and 4.98 + 0.28 mm. By comparison, the manual slice thickness method results were 4.71 + 0.39, 4.82 + 0.54, 4.89 + 0.50, and 4.79 + 0.43 mm (p-value 0.005, 0.291, 0.473, 0.452). The results of automated method for tube currents of 77, 154, 231, and 233 mA were 5.19 + 0.26, 4.98 + 0.28, 5.06 + 0.41, and 4.96 + 0.13 mm. By comparison, the results of manual slice thickness method were 4.42 + 0.34, 4.92 + 0.11, 4.72 + 0.37, and 4.80 + 0.46 mm (p-value 0.004, 0.642, 0.22, 0.75).

Conclusions: An automated slice thickness measurement on Neusoft CT the QA phantom image was successfully developed. The measurement results of

the automated method are closer to the set thickness than the manual method. The results of automatic slice thickness method are accurate for tube voltage, and tube current variations.

Keywords : Computed Tomography, Slice thickness, Image quality, Neusoft phantom

I. INTRODUCTION

Computed tomography (CT) is a leading medical imaging modality widely used worldwide to establish a diagnosis [1,2]. The success of diagnosis using CT strongly depends on the quality of the resulted images. Due to the complexity of CT which may lead to errors in resulted images and the use of ionizing radiation which may pose health risks in the future, hence routine CT quality control (QC) procedures to achieve accurate result and safe implementation of CT is needed [3]. By QC testing, any deviations or inconsistent results can be identified before the clinical examination [3].

One important parameter in CT is slice thickness. Slice thickness influences other important image parameters, such as noise and spatial resolution [4,5]. Increasing slice thickness can reduce image noise, however image resolution in z-axis decreases [6, 7]. Slice thickness of CT image can be less than 1 mm up to around 10 mm. In clinical setting, slice thickness has to be set carefully according to clinical demands [8]. Using an appropriate slice thickness will provide optimum image for specific diagnoses [9,10]. Therefore, the determination of the slice thickness must be appropriate for clinical purposes.

To achieve accurate slice thickness, its accuracy must be regularly checked [11,12]. In many CT centers, slice thickness measurements in a series of QC procedures rely on manual measurements using the tools available on the CT console [13]. Manual measurement is subjective, observer-dependent, and time-consuming [14]. Therefore, to obtain an objective, observer-independent, and fast measurement, an automated method is needed. Several researchers have developed automated systems to measure slice thickness on several available phantoms, such as the American Association of Physicists in Medicine (AAPM) CT performance phantom [15], American College of Radiology (ACR) CT accreditation phantom [16], and Catphan phantom [17].

In our hospital, we implemented Neusoft CT scanner. For routine QA, Neusoft CT QA phantom is always used [18]. It needs automatic system to achieve mentioned goals in our hospital. However, to the best of our knowledge, there is no tool for automatic QA, including for slice thickness measurement, for the Neusoft CT QA phantom. The study aimed at developing a software for automated measurement of slice thickness on Neusoft CT QA phantom. The results of automated measurements on variations of slice thickness, tube voltage, and tube current will be compared with manual measurements.

II. METHODS AND MATERIAL

A. Phantom description

The automated slice thickness measurement was developed on the Neusoft CT phantom (Figure 1). The phantom was a built-in phantom manufactured by Neusoft Medical System (Shenyang, China). The phantom consisted of 3 parts: head physical layer, head water layer, and body water layer. The phantom

case was made of acrylic material. The phantom was filled with purified water, which represented the content in the human body which mainly contains water [19]. These wire ramps were oriented parallel to the x-axis at 0° rotation. Table 1 indicates the phantom parts, functions, and composition.

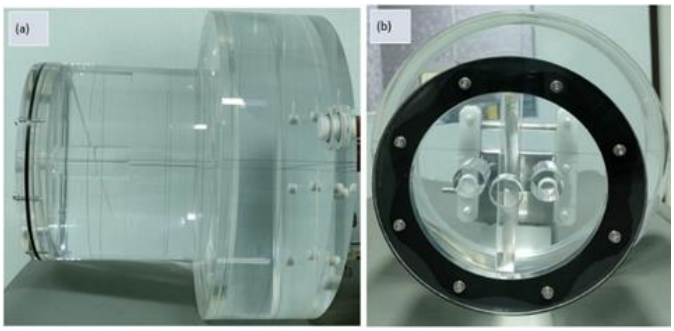

Figure 1. Photograph of the Neusoft CT QA phantom; (a) Side view, and (b) Front view

For slice thickness measurement, an aluminum ramp with an angle of 23° was provided in the head physical layer (Figure 2). The aluminum ramp was located within acrylic material. After correction with the angle, the profiles of the projections of the aluminum ramps in axial image were equivalent to the sensitivity profiles, and the full-width at half maximum (FWHM) of the profile indicated the slice thickness [20]. The diameter of the phantom was 200 mm with a PVC shell.

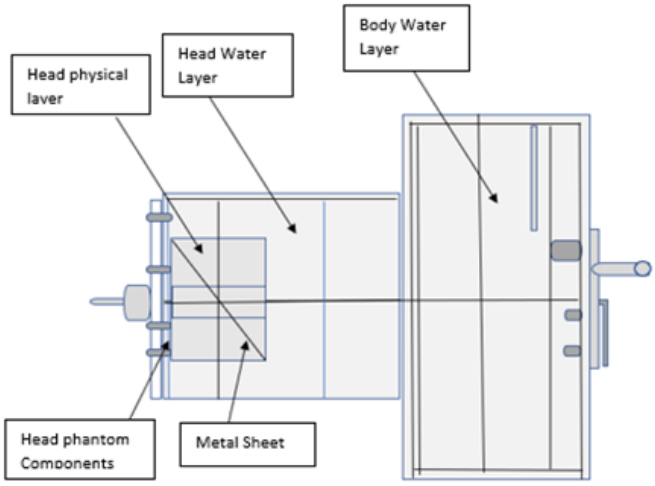

Figure 2. Geometry of the Neusoft CT QA phantom. Part for measuring slice thickness is located at head physical layer.

Table 1. Parts of the Neusoft CT QA phantom.

Phantom layer	Function	Composition
Head physical layer	Linear measurement	One linear measurement phantom: Acrylic
	Slice thickness measurement	Tilt Aluminum
	Air separation measurement	Fine copper wire
	Positioning accuracy measurement	Positioning balls
Head water layer	CT value, CT value uniformity, noise	Purified water
	Low contras resolution	
Body water layer	CT value	Purified water
	CT value uniformity	
	Noise	

B. Data acquisition

The phantom was scanned using the Neusoft NeuViz 16 Classic CT scanner (Neusoft Medical System, Shenyang, China) with the most common protocol in the QA procedure. The phantom was attached to the holder to avoid mis-centering. The scanning parameter settings for variations in slice thickness, tube voltage, and tube current were shown in Table 2.

The produced images were saved in (*Digital Imaging and Comunications in Medicine*) DICOM format. This axial DICOM image dataset was used to measure slice thickness. The measurements for all variations were repeated at 5 slices, except for the thickness of 10 mm, the measurements were only repeated at 4 slices because the resulting images were fewer.

C. Automated measurement process

The developed software for measuring slice thickness on Neusoft CT QA phantom has been integrated into IndoQCT software [21,22]. Figure 3 shows the graphical user interface (GUI) of IndoQCT for measuring slice thickness on the phantom. The steps of slice thickness measurement are depicted in Figure 4.

The process began with opening the original axial image of slice thickness part on the Neusoft CT QA phantom (Fig. 4a). Segmentation was performed with a threshold of 90 Hounsfield units (HU) to select the acrylic objects (Fig. 4b). The result of this segmentation was a binary image containing several acrylic objects (i.e. two circular acrylic object and one rectangular acrylic object). It is worth noting that the ramp object was located on a rectangle acrylic object. Thus, it is necessary to select a rectangular acrylic object. In this case, the labeling process was done (Fig. 4d). Rectangular acrylic object was selected based on the object's roundness level, and rectangular acrylic object was selected with the smallest roundness (Fig. 4d).

The next, a Hough transform was performed on the rectangular acrylic object. The Hough transform result was still in 2D (Fig. 4e). To automatically get the angle, the result of the 2D Hough transformation was converted to 1D by converting values greater than “0” to “1” and adding up in the y-axis direction. The angle of a rectangular acrylic object was then determined based on the minimum value of the 1D Hough transform results. Afterthat, the ramp object was segmented by the second thresholding method with a threshold value of 150 HU. Furthermore, the center of the ramp object was determined using the centroid equation.

Table 2. Scan parameters for slice thickness measurement for variations of slice thickness, tube voltage, and tube current.

Parameter	Variation		
	Slice thickness	Tube voltage	Tube current
Acquisition mode	Helical	Helical	Helical
Tube voltage (kV)	120	80, 100, 120, 140	120
Tube current (mA)	231	231	77, 154, 231, 233
Revolution time (s)	0.78	0.78	0.78
Scan Interval (mm)	20	20	20
FOV (mm)	345	370	356
Slice Thickness (mm)	1.25, 2.5, 3, 5, 10	5	5
Pitch	1.2	1.2	1.2
Filter	F20	F20	F20

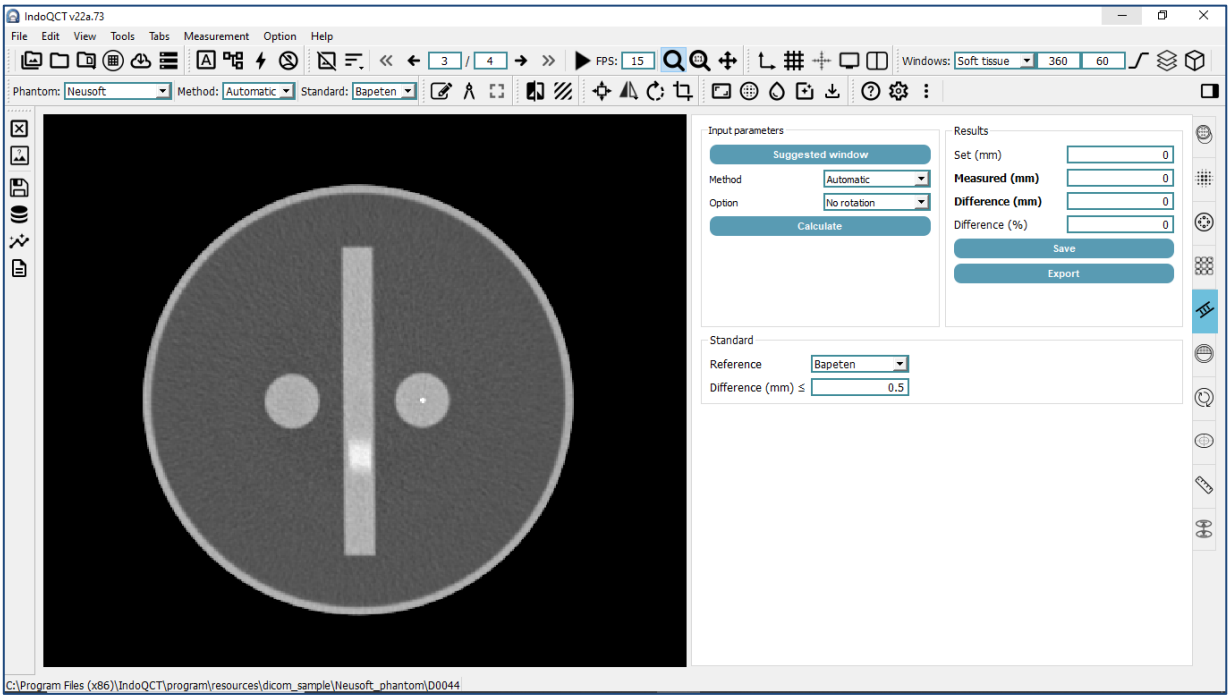

Figure 3. Graphical user interface (GUI) of IndoQCT for measuring slice thickness on the Neusoft CT phantom.

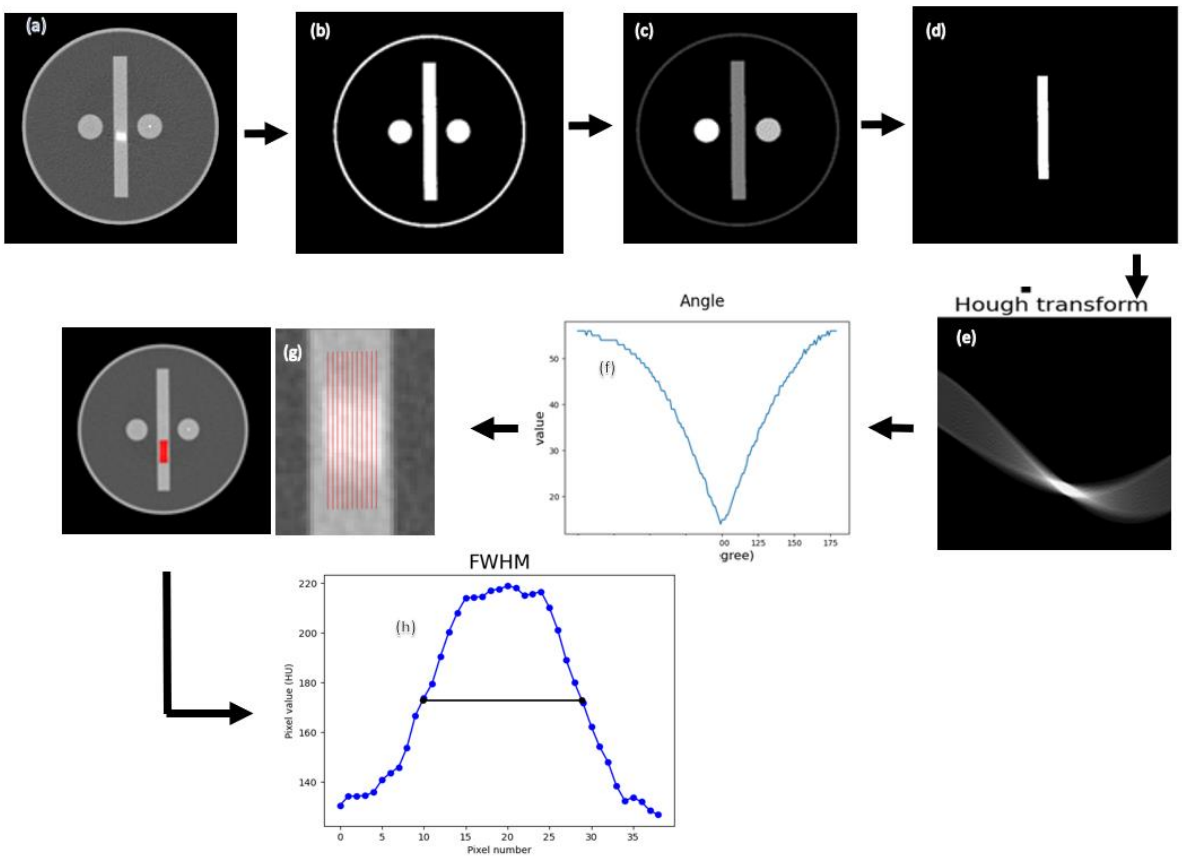

Figure 4. Automated slice thickness measurement process; (a) Original image, (b) Segmented acrylic objects within image (c) Labeled acrylic objects within image, (d) Rectangular acrylic object within image, (e) Result of Hough transform of rectangular acrylic object in 2D, (f) Results of transformation of 2D of Hough transform to 1D and detected angle was determined as the smallest value within this 1D graph, (g) Lines across the ramp object, and (h) Profile of the pixel values across the ramp object and it's FWHM

The obtained angle and center of the ramp objects were then used to place the lines precisely on the ramp object to find the profile across the ramp object (Fig. 4f). The pixel profiles obtained from this process were then averaged to anticipate noise (Fig. 4g). Finally, slice thickness was calculated by finding the FWHM of the average pixel profile, and multiplying it by the tangent of ramp object's slope (i.e. 23°) (Fig. 4h).

D. Manual measurement

In comparison to using automated slice thickness measurement results, manual measurements were also performed. The MicroDicom viewer was used to provide a ruler as a measuring tool. The results obtained were manually multiplied by the tangent of 23°. Figure 5 shows the image of the ramp object and the drawn line for measuring slice thickness manually. It appears that the boundary of the ramp object is very blurred so the upper and lower ends were determined subjectively.

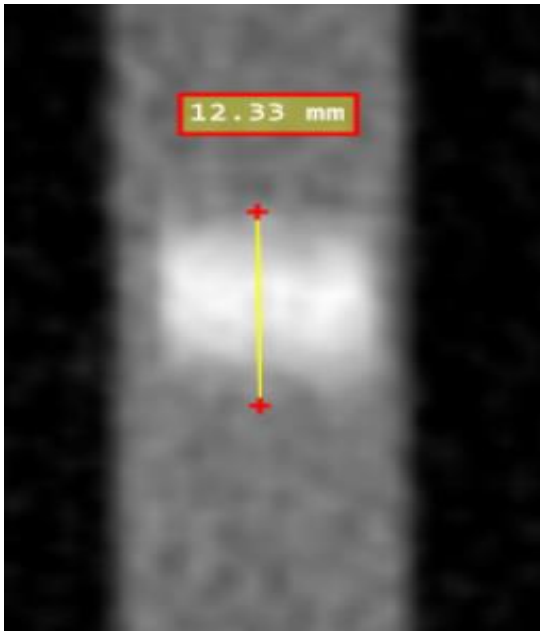

Figure 5. Manual measurement of slice thickness by a ruler of the MicroDicom viewer.

E. Data analysis

Resulted slice thickness measurement data were analyzed using the SPSS Versi 21 [23]. After knowing the value of the mean measured thickness in the automated and manual methods, the difference between both was determined. The significant difference between automated and manual measurement results was obtained by performing a t-test or independent t-test [24]. A t-test was applied to test the significance of the random sample mean, and the difference between the two sample means [25].

III.RESULTS AND DISCUSSION

A. Variation of slice thickness

Figure 6 shows images of phantom reconstructed with different slice thicknesses from 1.25 to 10 mm. On a small thickness slice, ramp object has a thin thickness, while on a large slice thickness it has a larger thickness. It appears that on a small slice thickness, ramp object appears brighter than the same object on a large slice thickness. Figure 7 shows the profiles across ramp object from automated measurements and their line FWHMs on a variation of slice thickness.

Table 3 shows the results of automatic slice thickness and manual measurements for various slice thickness. It appears that the results of slice thickness from automatic measurement are closer to the set slice thickness than manual measurement. For a slice thickness of 10 mm, the difference between the result of the automatic slice thickness and the set slice thickness is only 0.95 mm, while the difference between the result of the manual measurement and the set slice thickness is 1.34 mm. The linear relationships between set slice thickness with the slice thickness result from manual and automatic measurements are shown in Figure 8. It appears that the automatic measurement results have a value of R^2 (0.9988) greater than the manual measurement which is only 0.9546.

B. Variation of tube voltage

Figure 9 shows images of phantom acquired with different tube voltages of 80, 100, 120, and 140 kV. It appears that the greater the tube voltage, the smaller the image noise. In this tube voltage range, the segmentations of the ramp object are still accurate and produce accurate profiles across the ramp object.

Profiles across ramp object and their line FWHMs from automated measurements from four tube voltages are depicted in Figure 10.

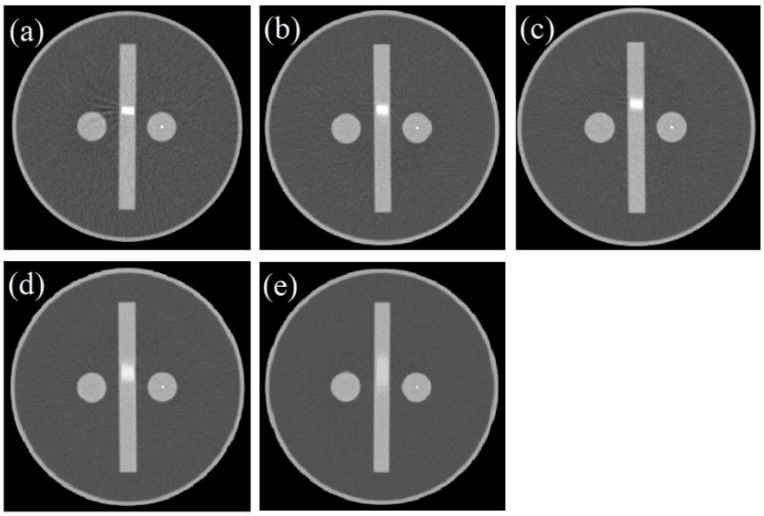

Figure 6. Axial images of phantom reconstructed for various slice thicknesses: (a) 1.25 mm, (b) 2.5 mm, (c) 3 mm, (d) 5 mm, and (e) 10 mm.

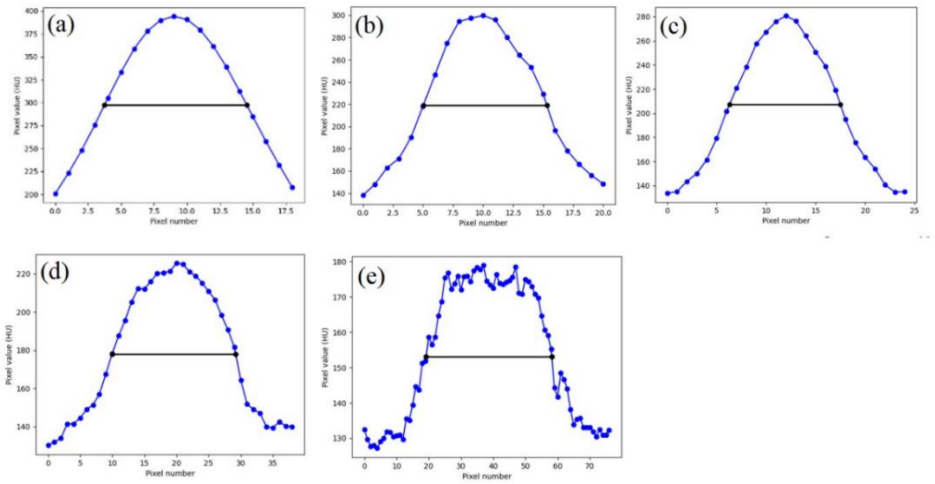

Figure 7 Profiles across ramp object from automated measurements and their line FWHMs for various slice thicknesses: (a) 1.25 mm, (b) 2.5 mm, (c) 3 mm, (d) 5 mm, and (e) 10 mm.

Table 3. Results of automatic slice thickness and manual measurements for various slice thickness from 1.25 to 10 mm.

Slice thickness (mm)	Automated		Manual		p-value
	measurement (mm)	Difference (mm)	measurement (mm)	Difference (mm)	
1.25	1.47 ± 0.169	0.22	2.91 ± 0.172	1.66	0.009
2.5	2.67 ± 0.08	0.17	3.28 ± 0.29	0.78	0.002
3	3.21 ± 0.17	0.21	3.57 ± 0.29	0.57	0.047
5	5.21 ± 0.13	0.21	4.72 ± 0.27	0.28	0.008
10	10.95 ± 0.28	0.95	11.34 ± 2.03	1.34	0.714

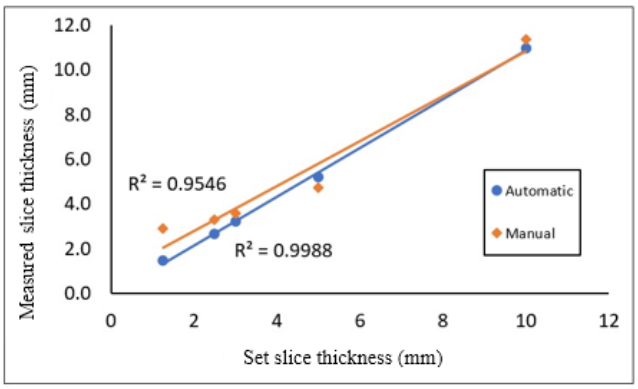

Figure 8. Linear relationships between set slice thickness with the measured slice thickness from manual and automatic measurements

Table 4 shows the results of automatic slice thickness and manual measurements for four tube voltages. It appears that the results of slice thickness from automatic measurement are comparable to those from manual measurements. The maximum difference between the slice thicknesses from the automatic measurement is 0.61 mm at 80 kV, and the maximum difference between the slice thicknesses from the manual measurement is 0.29 mm at 80 kV. A significant difference between the automated and manual measurements at 80 kV, with a p-value of 0.005. Meanwhile, for 100, 120, and 140 kV, there was no significant difference between automated and manual measurements respectively with p-values of 0.291, 0.473, and 0.452.

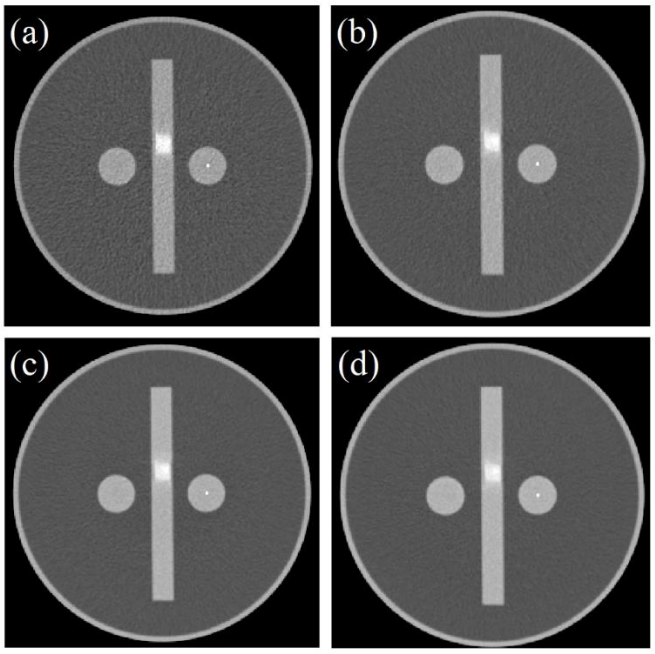

Figure 9. Axial images of phantom reconstructed for various tube voltages: (a) 80 kV, (b) 100 kV, (c) 120 kV, and (d) 140 kV.

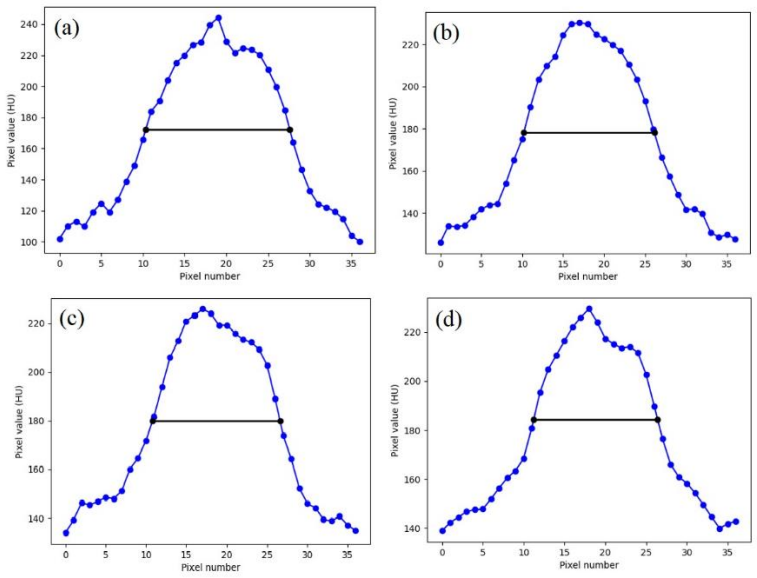

Figure 10. Profiles across ramp object from automated measurements and their line FWHMs for various tube voltages: (a) 80 kV, (b) 100 kV, (c) 120 kV, and (d) 140 kV.

Table 4. Results of automatic slice thickness and manual measurements for various tube voltages from 80 to 140 kV.

Tube Voltage (kV)	Slice Thickness (mm)	Automated		Manual		p-value
		Measurement (mm)	Difference (mm)	Measurement (mm)	Difference (mm)	
80	5	5.61± 0.34	0.61	4.71 ± 0.39	0.29	0.005
100		5.12 ± 0.23	0.12	4.82 ± 0.54	0.18	0.291
120		5.08 ± 0.23	0.08	4.89 ± 0.50	0.11	0.473
140		4.98 ± 0.28	0.02	4.79 ± 0.43	0.21	0.452

C. Variation of tube current

Figure 11 shows images of phantom acquired with different tube currents of 77, 154, 231, and 233 mA. It appears that the greater the tube current, the smaller the image noise as expected. Furthermore, in this tube current range, the segmentations of the ramp object are still accurate and produce accurate profiles across the ramp object. Profiles across ramp object and their line FWHMs from automated measurements from four tube voltages are depicted in Figure 12. Table 6 shows the results of automatic slice thickness and manual measurements for four tube currents. It appears that the results of slice thickness from automatic measurement are comparable to those from manual measurements. The maximum difference between the slice thicknesses from the automatic measurement is 0.19 mm at 77 mA, and the manual measurement is 0.58 mm at 77 mA. A significant difference between the automated and manual measurements at 77 mA, with a p-value of 0.004.

This study is for developing an automated slice thickness measurement on Neusoft CT QA phantom images. We evaluated the system with variations in slice thickness, tube voltage, and tube current. The consideration for choosing these parameters was motivated by frequent changes in the parameters of slice thickness, tube voltage, and tube current according to the type of CT scan examination. The developed software must be able to measure slice thickness accurately for these various variations commonly used in daily practice.

We found that, in general, the developed software was able to detect slice thickness accurately for the three variations used. When compared with manual measurements, the results of automatic slice thickness measurements are closer to the set slice thickness as shown in Tables 3, 4 and 5.

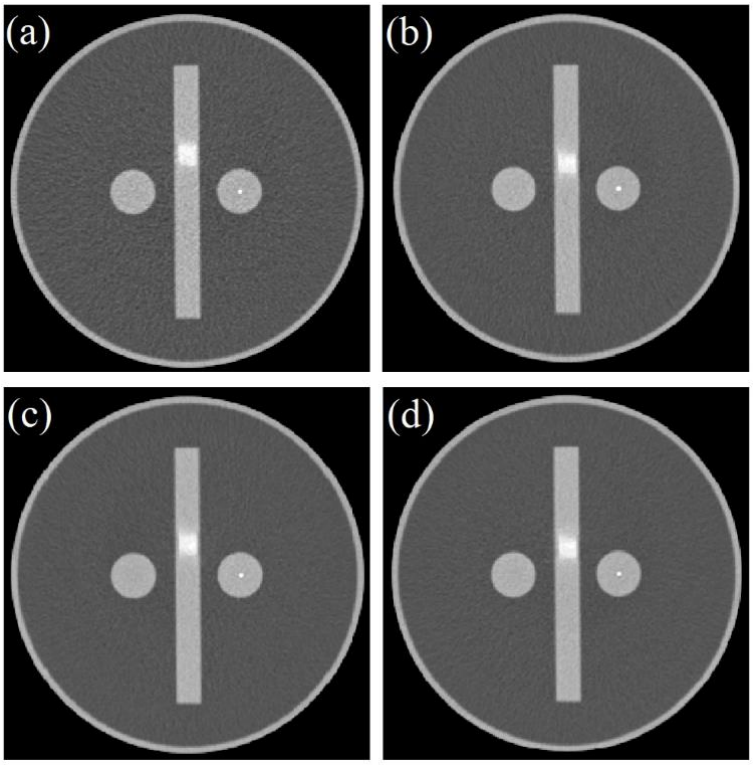

Figure 11. Axial images of phantom reconstructed for various tube currents: (a) 77 mA, (b) 154 mA, (c) 231 mA, and (d) 233 mA

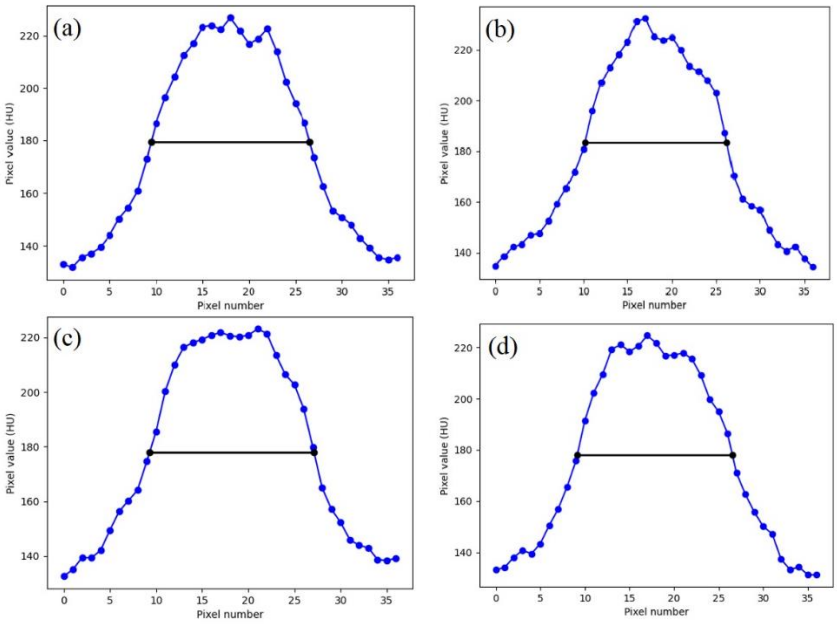

Figure 12. Profiles across ramp object from automated measurements and their line FWHMs for various tube currents: (a) 77 mA, (b) 154 mA, (c) 231 mA, and (d) 233 mA.

Table 5. Results of automatic slice thickness and manual measurements for various tube currents from 77 to 233 mA.

Tube current (mA)	Set Thickness (mm)	Automated		Manual		p-value
		Measurement (mm)	Difference (mm)	Measurement (mm)	Difference (mm)	
77	5	5.19 ± 0.26	0.19	4.42 ± 0.34	0.58	0.004
154		4.98 ± 0.28	0.02	4.92 ± 0.11	0.08	0.642
231		5.06 ± 0.41	0.06	4.72 ± 0.37	0.28	0.223
233		4.96 ± 0.13	0.04	4.80 ± 0.46	0.20	0.750

It is noted that manual measurements are very subjective. The upper and lower limits of the ramp object are blurred, so that the determination of the slice thickness visually depends on the expertise and experience of the observer. The smaller the slice thickness, accuracy to obtain slice thickness manually becomes more difficult. From this research, it was found that at large slice thicknesses, the measured slice thickness results tend to be accurate, while at small slice thicknesses, the measurement results are less accurate as shown in Figure 8 and Table 3.

The independent t-statistical test results were also obtained showing that there were no significant differences ($p > 0.05$) for all variations between automatic and manual measurements, except for the small slice thickness (1.25, 2.5, 3, and 5 mm), the smallest voltage (80 kV) and the smallest current (77 mA). Manual measurements appear to be further away from the set slice thickness if slice thickness is getting smaller. This does not occur in the results of automatic measurements. The automatic measurement results still show accurate even at small slice thicknesses.

The developed algorithm for measuring slice thickness on the Neusoft CT QA phantom has been equipped with ability to adapt to variations of the phantom rotation angle and field of view (FOV). However, in this study we have not tested the ability of the algorithm to measure slice thickness at various phantom rotation angles and FOV variations.

Although the developed algorithm is able to accurately measure the slice thickness for tube voltage from 80 kV and tube currents from 77 mA, however, for smaller tube currents there is a possibility that the automatic slice thickness detection will not be successful. Therefore, testing this algorithm for a large variety of noise needs to be done. Testing algorithm for other Neusoft CT scanners also needs to be done, because in this study, testing was only carried out on one CT machine.

IV.CONCLUSION

An automated slice thickness measurement on Neusoft CT the QA phantom image was successfully developed. The measurement results of the automated measurement are closer to the set thickness than the manual method. In manual measurement, measured slice thickness increasingly differs from the set slice thickness for the small slice thickness. However, this does not occur in the results of automatic slice thickness measurements. The results of automatic slice thickness measurements are accurate for tube voltage and tube current variations.

V. REFERENCES

[1]. Samei E, Pelc JJ. Computed Tomography. Springer. 2020.

[2]. American College of Radiology. Computed Tomography Quality Control Manual. 2017.

[3]. Dillon C, Breeden W, Clements J, et al. American College of Radiology. Computed Tomography. Quality Control Manual. 2017.

[4]. Ni Putu Rita Jeniyanthi. The effect of slice thickness variations on the quality of the image

and value bleeding volume on DSCT brain examination. International Journal of Allied Medical Sciences and Clinical Research, 8(2), 251-257. Retrieved from https://ijamscr.com/ijamscr/article/view/859. 2020

[5]. Samsun S, Prananto L, Wulandari N. Image quality differences in CT scan thorax by using slice thickness variation. SANITAS: Jurnal Teknologi dan Seni Kesehatan. 2017;8(2):87-91.

[6]. International Atomic Energy Agency. Quality assurance programme for computed tomography: Diagnostic and therapy applications. IAEA Human Health Series No˚19, IAEA, Vienna. 2012.

[7]. Kim YJ, Lee HJ, Kim HG, Lee SH. Research Article: The effect of CT scan parameters on the measurement of CT radiomic features: A lung nodule phantom study. Computational and Mathematical Methods in Medicine. 2019;2019;8790694.

[8]. Ford JM, Decker SJ. Computed tomography slice thickness and its effects on three-dimensional reconstruction of anatomical structures. Journal of Forensic Radiology and Imaging. 2016;4:43-46.

[9]. Dowsett DJ, Kenny PA, Johnston RE. The physics of diagnostic imaging. Second edition. 2006.

[10]. Luo H, He Y, Jin F, et al. Impact of CT slice thickness on volume and dose evaluation during thoracic cancer radiotherapy. Cancer Manag Res. 2018;10:3679-3686.

[11]. Monnin P, Sfameni N Gianoli A, Ding S. Optimal slice thickness for object detection with longitudinal partial volume effects in computed tomography. J Appl Clin Med Phys. 2017;18(1):251-259.

[12]. Makmur IWA, Setiabudi W, Anam C. Evaluasi ketebalan irisan (slice thickness) pada pesawat CT scan single slice. Jurnal Sains dan Matematika. 2013;21(2):42-47.

[13]. Giuseppe Vermiglio, Giuseppe Acri, Barbara Testagrossa, 2011. Procedure for Evaluation of slice thickness in Medical Imaging systems. Modern Approaches to quality control DOI : 10.5772/23693. InTech Open, London: Nov 2011.

[14]. Sofiyatun S, Anam C, Zahra UM, Rukmana DA, Dougherty G. An automated measurement of image slice thickness of computed tomography. Atom Indonesia. 2021;47(2):121-128.

[15]. Lasiyah N, Anam C, Hidayanto E, Dougherty G. Automated procedure for slice thickness verification of computed tomography images: Variations of slice thickness, the position from iso center and reconstruction filter. J Appl Clin Med Phys. 2021;22(7):313-321.

[16]. Hobson MA,Soisson ET, Davis SD, Parker W. Using the ACR CT accreditation phantom for routine image quality assurance on both CT and CBCT imaging systems in a radiotherapy environment. J Appl Clin Med Phys. 2014;15(4):4835.

[17]. Jiang H. Computed Tomography Principles, Design, Artifact and Recent Advances Second Edition. Publish by SPIE Bellingham, Washington. 2009.

[18]. Njiki CD, Ma-you JEMN, Yigbedeck YE, Abou'ou DW, Yimele BC, Sabouang JF. Assessment of image quality parameters for computed tomography in the City of Yaoundé. Open Journal of Radiology. 2018;8:37-44.

[19]. Popkin BM, D'Anci KE, Rosenberg IH. Water, hydration, and health. Nutr Rev. 2010;68(8):439-58.

[20]. Multi-slice CT Scanner System NeuViz 16 Classic User Manual (Vol 1) Neusoft Medical System Co., Ltd. No. 177-1 Chuangxin Road, Hunnan District, Shenyang, Liaoning, China 110167. Https://medical.neusoft.com.

[21]. Anam C, Naufal A, Fujibuchi T, Matsubara K, Dougherty G. Automated development of the contrast-detail curve based on statistical low-

contrast detectability in CT images. J Appl Clin Med Phys. 2022;23(9):e13719.

[22]. Anam C, Naufal A, IndoQCTv22a: Software for evaluating the quality of computed tomography images. Technical report December 2022.

[23]. Arkkelin Daniel, "Using SPSS to understand Research and Data Analysis" (2014). Physchology Curricular Materials.1. https://scholar.valpo.edu/psych_oer/1

[24]. Kim TK. T test as a parametric statistic. Korean J Anesthesiol. 2015;68(6):540-6.

[25]. Gerald B. A brief review of independent, dependent and one sample t-test. International Journal of Applied Mathematics and Theoretical Physics. 2018;4(2):50-54.

Cite this Article

Rini Marini, Choirul Anam, Eko Hidayanto, Ariij Naufal, Geoff Dougherty, "Automated Slice Thickness Measurement on the Nessoft CT QA Phantom", International Journal of Scientific Research in Science and Technology (IJSRST), Online ISSN : 2395-602X, Print ISSN : 2395-6011, Volume 10 Issue 3, pp. 472-484, May-June 2023. Available at doi : https://doi.org/10.32628/IJSRST52310386
Journal URL : https://ijsrst.com/IJSRST52310386